A Two-Stage Distributionally Robust Optimization Model for Wind Farms and Storage Units Jointly Operated Power Systems

PANPAN LI[1,2], **(Graduate Student Member, IEEE), LIANGYUN SONG**[1,2], **JIXIAN QU**[1],
YUEHUI HUANG[1], **(Senior Member, IEEE), XIAOYUN WU**[3], **XI LU**[4],
AND SHIWEI XIA[1,2], **(Senior Member, IEEE)**

[1]State Key Laboratory of Operation and Control of Renewable Energy & Storage Systems (China Electric Power Research Institute), Beijing 100085, China
[2]School of Electrical & Electronic Engineering, North China Electric Power University, Beijing 102206, China
[3]College of Mechanical and Optoelectronic Physics, Huaihua University, Huaihua 418000, China
[4]School of Electrical Engineering, Southeast University, Nanjing 210096, China

Corresponding authors: Xiaoyun Wu (wuxiaoyun111@126.com) and Shiwei Xia (s.w.xia@ncepu.edu.cn)

ABSTRACT To explore the benefit of energy storage for countering high-level wind power fluctuations, a two-stage distributionally robust optimization model is proposed for wind farms and storage units (SUs) jointly operated power systems. First, the 1-norm and ∞-norm confidence sets are presented to model the fluctuations of wind power output, then a two-stage distributionally optimization model is formed to minimize system total cost with secure operation constraints, where the ON-OFF status of generators and SUs are determined in the first stage by day-ahead dispatching, while the power output of generators, wind power curtailment, load shedding and SUs charging/discharging power are optimized in the second stage. Afterward, the column-and-constraint generation (CCG) algorithm is presented to solve the proposed two-stage model. Finally the influence of confidence level of confidence sets and SU capacities on system total cost is analyzed, and the effectiveness of the proposed model is also validated by the case studies.

INDEX TERMS Distributionally robust optimization, CCG algorithm, two-stage, confidence set, storage units.

NOMENCLATURE

T	Dispatching period
G	Number of generators
S	Number of storage units (SUs)
D	Number of loads
W	Number of wind farms
K	Number of branches
$z_{g,t} v_{g,t} u_{g,t}$	Binary variables, $z_{g,t} = 1$ stands for generator g at time t in started up status; $v_{g,t} = 1$ stands for the generator g at time t in shut down status; $u_{g,t} = 1$ stands for the generator g at time t is ON, otherwise OFF
$I_{s,t}^{sc}, I_{s,t}^{sd}$	Binary variables, $I_{s,t}^{sc} = 1$ and $I_{s,t}^{sd} = 1$ mean SU s is charging and discharging at time t respectively
$S_{g,u}$	Start-up cost of generator g
$S_{g,d}$	Shut-down cost of generator g
c_s	Energy cycling cost of SU s
T_g^{on}	Minimum up-time of generator g
T_g^{off}	Minimum down-time of generator g
P_n	Probability of scenario n
$P_{g,t}$	Power output of generator g at time t
$\Delta w_{w,t}$	Wind power curtailment of wind farm w at time t
$\Delta D_{d,t}$	Load shedding of load d at time t
$p_{s,t}^{sd}$	Discharging power of SU s at time t
$p_{s,t}^{sc}$	Charging power of SU s at time t
$\lambda_{w,t}$	Wind curtailment penalty price of wind farm w at time t
$\lambda_{d,t}$	Load shedding penalty price of load d at time t

The associate editor coordinating the review of this manuscript and approving it for publication was Gaetano Zizzo.

c_{sd}	Price of discharging power of SU s
c_{sc}	Price of charging power of SU s
P_g^{min}	Minimum output power of generator g
P_g^{max}	Maximum output power of generator g
R_{Ug}	Ramp-up limit of generator g
R_{Dg}	Ramp-down limit of generator g
F_{ij}^{max}	Thermal capacity of transmission line ij
K_{ij}^b	Flow distribution factor of transmission line ij
B	Set for all buses
S_b	SU Set at bus b
G_b	Generator set at bus b
w_b	Wind farm set at bus b
D_b	Load demand set at bus b
$p_{min}^{sd}, p_{max}^{sd}$	Minimum/maximum discharging power of SU s
$p_{min}^{sc}, p_{max}^{sc}$	Minimum/maximum charging power of SU s
$SOC_{s,min}, SOC_{s,max}$	Minimum/maximum capacity of SU s
$p_{s,t}^{sd}, p_{s,t}^{sc}$	Charging/discharging power of SU s at time t
$SOC_{s,t}$	State of Charge of SU s at time t
$SOC_{s,1}$	Initial State of Charge of SU of the Dispatching Period
$SOC_{s,T}$	Finale State of Charge of SU of the Dispatching Period
η_c, η_d	Charging and discharging efficiency
$Q_{s,rate}$	Rated energy capacity of SU s

I. INTRODUCTION

Due to the high volatility and limited prediction accuracy of renewable energy, wind power curtailment is still a main concern for power system operation. In order to enhance the accommodation level of wind power and realize the optimal operation of power systems with uncertain wind power, the cooperated operation of SUs and wind farms is promising to effectively harvest wind power and improve system operation economics.

There are two typical approaches to handle uncertainties of wind power output including the stochastic optimization (SO) method and robust optimization (RO) method. SO generates a large number of scenarios based on the probability density function of uncertain variables, and afterward transforms the stochastic optimization problem into a large set of deterministic problems by scenario generation and reduction techniques. Since it is difficult to obtain the exact probability density function of uncertain variables in practice and the calculation burden of SO also increases significantly with the growing number of scenarios, consequently RO is developed. In contrast, the RO method does not need the specific probability density function of uncertain variables and usually utilizes the interval sets to describe the upper and lower boundary of uncertain variables. However, as RO tries to make optimal decisions in the worst scenarios, its solutions are often very conservative. To overcome the shortcomings of the RO and SO method, a two-stage stochastic optimization model was implemented in [1]. [2]–[4] constructed a

multi-band uncertainty set considering the temporal correlation to describe the wind/load prediction error which reduced the conservativeness of the robust unit commitment model.

In recent years, as a hybrid variant of RO and SO, the distributionally robust optimization (DRO) model attracted much attention and was researched for power system operation [5]–[7]. Based on the assumption that random variables satisfy a large set of a probability distribution, DRO would find robust decisions for the worst probability distribution in an ambiguity set or a confidence set. As the conservativeness and accuracy of the DRO solution are closely dependent on the formation of an ambiguity set, how to model the ambiguity set is the key of DRO model, which could be divided into two branches. 1) The first is a moment-based method. In [8], an ambiguity set is used to capture the uncertainty of wind power based on moment information, and a DRO model for unit commitment problem is addressed by affine approximation algorithm. 2) The second defined DRO ambiguity set contains all distributions within a distance from the nominal distribution. Compared with the moment-based method, the distance-based method obtains more valuable information from the available historical data of uncertainties. [9], [10] describe uncertain variables by distance-based ambiguity set and the model is solved by a decomposition algorithm which shows a good performance in terms of computation efficiency.

The above works made contributions to reducing the computational complexity and improving the conservations of power system optimal operation with uncertain renewables. However, there is still a lack of research on the effective reduction of wind power curtailment levels. In order to further deal with the wind curtailment problem and guarantee system reliability, the SU is reorganized to apply with the electric power system because of its ability to provide reasonable charging or discharging behaviors. Reference [11] proposed a two-stage DRO model for energy and reserve dispatch under a set of probability distributions with known means and variances. Reference [12] collected the moment information from wind power historical data and established an optimal operation model for a wind power-heat hybrid system, afterward effectively solved the model by S-lemma theory. By using the distance-based ambiguity sets, the dispatching cost of a hybrid system was minimized by DRO in [13]–[15]. Reference [16] applied Kernel density estimation to construct an ambiguous probability distribution of wind power uncertainty and finally built up a DRO model for energy and reserve optimization. However as the DRO model with distance-based ambiguity set is usually a three-level programming problem, it is usually intractable to be directly solved. Recently, a data-driven DRO model that used the 1-norm or ∞-norm confidence set for accommodating possible probabilistic distribution of concerned random variables was proposed in [17] and later used in transmission planning, energy storage management, and reactive power optimization [18]–[21]. To sum up, the moment-based DRO model is usually conservative for power system coordinated

operation [22]–[24] while the distance-based DRO model is with high computational complexity [25], [26].

To address conservatism and calculation issues, a two-stage DRO model is established for wind farms and storage units jointed operated power systems, where the 1-norm and ∞-norm confidence set is used to describe the uncertain wind power output and taken into account in DRO constraints. In the first stage, the ON-OFF status of generators and SUs are determined by day-ahead dispatching, while generators' power output, wind power curtailment and load shedding amount are optimized in the second stage according to representative scenarios of uncertain wind power. In order to effectively solve the proposed model, the column-and-constraint generation (CCG) algorithm is adopted to decompose the proposed model into a master problem and sub-problems which were addressed iteratively. Finally, the effectiveness of the proposed two-stage DRO model is verified by the numerical simulation. The main contributions of the paper are two-fold as follows.

1) The uncertain wind power output is first modeled by the 1-norm and ∞-norm confidence set, and a two-stage distributionally robust optimization model (DRO) is proposed for wind farms and storage units jointly operated power systems, which can compromise the operation conservative and economic of the jointed system. Consequently, the CCG decomposition method is also applied to efficiently solve the proposed model.

2) Simulation results of a modified New England 39-bus system have validated the effectiveness of the proposed DRO model for wind farms and storage units jointed power system economic operation; the influence of confidence level of norm confidence set, the historical data volume, and SUs capacities on system total cost are also analyzed comprehensively in the case studies.

The paper is organized as follows. Section II introduces the norm confidence set and proposes the two-stage DRO model for wind farms and storage units jointly operated power systems, while Section III and IV apply the linearization technique and CCG algorithm to solve the proposed model. In section V, the 39-bus, 57-bus and 118-bus systems are tested to validate the effectiveness of the proposed model. Finally, the conclusion is drawn in the last section.

II. TWO-STAGE DISTRIBUTIONALLY ROBUST OPTIMIZATION MODEL UNDER THE NORM CONFIDENCE SET

In this section, the two-stage DRO model based on the 1-norm and ∞-norm confidence set is built for wind farms and SUs coordinated operation, in which the start-up and shut-down cost, the generation cost, the wind curtailment and load shedding cost are considered in the objective, meanwhile the generator output limits and ramp up/down limits, transmission line thermal capacity, wind curtailment and load shedding limits, etc. are considered as operational constraints.

A. NORM CONFIDENCE SETS FOR DRO MODEL

According to [17], assume N discrete scenarios obtained from K observations (the corresponding probability distribution of each scenario is p_n^0 based on the empirical distribution) which are used to represent the uncertain wind power output. And considering the actual probability distribution may deviate from the historical empirical distribution, with the pre-settled parameter θ_1 and θ_∞, the 1-norm and ∞-norm based confidence sets are defined as:

$$D_1 = \left\{ P \in \mathbb{R}_+^N \mid \|P - P_0\|_1 \leq \theta_1 \right\}$$
$$= \left\{ P \in \mathbb{R}_+^N \mid \sum_{n=1}^N \left| p_n - p_n^0 \right| \leq \theta_1 \right\} \quad (1)$$

$$D_\infty = \left\{ P \in \mathbb{R}_+^N \mid \|P - P_0\|_\infty \leq \theta_\infty \right\}$$
$$\left\{ P \in \mathbb{R}_+^N \mid \max_{1 \leq n \leq N} \left| p_n - p_n^0 \right| \leq \theta_\infty \right\} \quad (2)$$

where $P = [p_1, p_{2,...}, p_n]$ is the actual distribution vector of uncertain variables, $P_0 = [p_1^0 \ldots . p_N^0]$ represents the empirical distribution vector of uncertain variables.

The relationship between P and P_0 under the 1-norm or ∞-norm confidence set is:

$$\Pr \left\{ \|P - P_0\|_1 \leq \theta_1 \right\} \geq 1 - 2N \cdot \exp\left(-2K\theta_1/N\right) \quad (3)$$
$$\Pr \left\{ \|P - P_0\|_\infty \leq \theta_\infty \right\} \geq 1 - 2N \cdot \exp\left(-2K\theta_\infty\right) \quad (4)$$

The right side of (3)-(4) represents the required confidence levels, if they are denoted by α_1 and α_∞, (5) and (6) can be obtained.

$$\theta_1 = \frac{N}{2K} \ln \frac{2N}{1 - \alpha_1} \quad (5)$$

$$\theta_\infty = \frac{1}{2K} \ln \frac{2N}{1 - \alpha_\infty} \quad (6)$$

From (5)-(6), it is noted that with a growing number of sample data K, the corresponding θ_1 and θ_∞ gradually approach zero and the confidence set (1)-(2) ensures the empirical distribution much closer to the actual distribution of uncertain variables. Moreover for the same confidence level ($\alpha_1 = \alpha_\infty$), θ_1 is larger than θ_∞, and accordingly (5) will be more conservative than (6) since the former would address more fluctuations of uncertain variables. The combined 1-norm and ∞-norm confidence set is formulated as (7) [27], [28].

$$D = \left\{ p_n \left| \begin{array}{c} p_n \geq 0 \\ \sum_{n=1}^N P p_n = 1 \\ \sum_{n=1}^N \left| p_n - p_n^0 \right| \leq \theta_1 \\ \max_{1 \leq n \leq N} \left| p_n - p_n^0 \right| \leq \theta_\infty \end{array} \right. \right\} \quad (7)$$

B. FIRST STAGE OF THE PROPOSED DRO MODEL

In the first stage, the day-ahead dispatching model is formulated to minimize the total generator start-up/shut-up cost by optimizing the ON-OFF status of generators. The first stage variables are strictly decided day-ahead which is not influenced by the uncertainty.

The objective in the first stage is expressed as (8).

$$\min \sum_{t=1}^{T} \sum_{g=1}^{G} \left(S_{g,u} z_{g,t} + S_{g,d} v_{g,t} \right) \tag{8}$$

The constraints include the following:

$$u_{g,t} - u_{g,t-1} \leq z_{g,t} \quad \forall g \in G, \forall t \in T \tag{9}$$

$$u_{g,t-1} - u_{g,t} \leq v_{g,t} \quad \forall g \in G, \forall t \in T \tag{10}$$

$$z_{g,t} + v_{g,t} \leq 1 \quad \forall g \in G, \forall t \in T \tag{11}$$

$$\left(u_{g,(t+1)} - u_{g,t} \right) T_g^{on} - \sum_{k=t+2}^{\min\{t+T_g^{on},T\}} u_{g,k} \leq \max\{1, T_g^{on} - T + t - 1\} \quad \forall g \in G, \forall t \in 1, 2, \ldots, T-2 \tag{12}$$

$$\left(u_{g,(t+1)} - u_{g,t} \right) T_g^{off} - \sum_{k=t+2}^{\min\{t+T_g^{off},T\}} u_{g,k} \leq T_g^{off}$$
$$\forall g \in G, \forall t \in 1, 2, \ldots, T-2 \tag{13}$$

In the above, Eqs. (9)-(11) are generator start-up and shut-down operational constraints based on its ON-OFF status $u_{g,t}$; Eqs. (12) and (13) represent the minimum up and down hours for each generator.

C. SECOND STAGE OF THE PROPOSED DRO MODEL

In the second stage, with consideration of uncertain variables, the generator power output, wind power curtailment, load shedding and SU charging/discharging power are optimized. And the second stage decision variables can be flexibly adjusted for each wind output scenario to minimize the dispatching cost under the worst-case scenario correspond to the uncertain wind power output.

$$\max_{P_n \in D} \min_{P_{g,t}, \Delta w_{w,t}, \Delta D_{d,t}, p_{s,t}^{sd}, p_{s,t}^{sc}} \sum_{n=1}^{N} P_n * \left[\sum_{g=1}^{G} \sum_{t=1}^{T} f_g(P_{g,t}) \right.$$
$$+ \sum_{w=1}^{W} \sum_{t=1}^{T} \lambda_{w,t} \Delta w_{w,t} + \sum_{d=1}^{D} \sum_{t=1}^{T} \lambda_{d,t} \Delta D_{d,t}$$
$$\left. + \sum_{s=1}^{S} \sum_{t=1}^{T} \left(c_{sd} p_{s,t}^{sd} + c_{sc} p_{s,t}^{sc} \right) \right]^n \tag{14}$$

where D is the hybrid 1-norm and ∞-norm confidence set defined by (7); $f_g(P_{g,t}) = a_g P_{g,t}^2 + b_g P_{g,t} + c_g$ is the generation cost in quadratic form and a_g, b_g, c_g are the fuel cost coefficients. $\lambda_{w,t} \Delta w_{w,t}$ is the wind curtailment cost of wind farm w at the time t; $\lambda_{d,t} \Delta D_{d,t}$ is the load shedding cost of load d at time t. $c_{sd} p_{s,t}^{sd}$ and $c_{sc} p_{s,t}^{sc}$ stand for the charging and discharging cost of SU s at time t. As the frequent charging/discharging cycles of SU would significantly affect the lifetime of a battery, and thus the battery lifecycle constraint is considered in the model. As indicated by experiments in [28] and [29], the most primary determinant on battery life is the depth of discharge (Dod) or State of Charge (SOC), and ESS lifetime could be approximately predicted for a given Dod or SOC. With the SOC constraint (25) in our paper, the ESS lifetime is approximated as fixed years, and afterward, the battery lifecycle degradation cost is amortized for the total cost including the one-time installation cost, annual operation and maintenance cost, and consequently, the battery limited lifecycle is indirectly considered in the

charging/discharging power price (c_{sd} or c_{sd}) of a battery energy storage unit.

The operation constraints include the following.

$$u_{g,t} P_g^{min} \leq P_{g,t} \leq u_{g,t} P_g^{max} \forall g, \forall t \tag{15}$$

$$\begin{cases} P_{g,t} - P_{g,t-1} \leq R_{Ug} u_{g,t-1} + P_g^{max} (1 - u_{g,t-1}) \\ P_{g,t-1} - P_{g,t} \leq R_{Dg} u_{g,t} + P_g^{max} (1 - u_{g,t}) \end{cases} \tag{16}$$

$$-F_{ij}^{max} \leq \sum_{b \in B} K_{ij}^b \left(\sum_{g \in G_b} P_{g,t} + \sum_{s \in S_b} \left(p_{s,t}^{sd} - p_{s,t}^{sc} \right) \right.$$
$$\left. + \sum_{w \in w_b} (W_{w,t} - \Delta W_{w,t}) - \sum_{d \in D_b} (D_{d,t} - \Delta D_{d,t}) \right) \leq F_{ij}^{max} \tag{17}$$

$$\sum_{b \in B} \left[\sum_{g \in G_b} P_{g,t} + \sum_{s \in S_b} \left(p_{s,t}^{sd} - p_{s,t}^{sc} \right) + \sum_{w \in w_b} (W_{w,t} \right.$$
$$\left. - \Delta W_{w,t}) \right] = \sum_{b \in B} \sum_{d \in D_b} (D_{d,t} - \Delta D_{d,t}) \tag{18}$$

$$0 \leq \Delta W_{w,t} \leq W_{w,t} \tag{19}$$

$$0 \leq \Delta D_{d,t} \leq D_{d,t} \tag{20}$$

$$I_{s,t}^{sd} p_{min}^{sd} \leq p_{s,t}^{sd} \leq I_{s,t}^{sd} p_{max}^{sd} \tag{21}$$

$$I_{s,t}^{sc} p_{min}^{sc} \leq p_{s,t}^{sc} \leq I_{s,t}^{sc} p_{max}^{sc} \tag{22}$$

$$I_{s,t}^{sd} + I_{s,t}^{sc} <= 1 \tag{23}$$

$$\left. \begin{array}{l} SOC_{s,t} = SOC_{s,t-1} + \left(p_{s,t}^{sc} \eta_c - \dfrac{p_{s,t}^{sd}}{\eta_d} \right) / Q_{s,rate} \\ SOC_{s,T} = SOC_{s,1} \end{array} \right\} \tag{24}$$

$$SOC_{s,min} \leq SOC_{s,t} \leq SOC_{s,max} \tag{25}$$

In the above formulation, (15) limits the maximum/minimum power output of generator g. (16) represents the ramping up/down capacity limits of generator g. (17) is the thermal capacity constraint for transmission line ij. (18) ensures power balance constraint. The upper and lower bounds of wind power curtailment and load shedding are enforced by (19-20). Constraints (21-22) define the maximum/minimum charging/discharging power limits of SU. (23) is the mutually exclusive conditions for the charging and discharging status. Constraint (24) represents the state of charge (SOC) of SU s during successive hours. The amount of SOC is limited in (25).

In addition, since the scenarios representing the uncertainties in sub-problems (15)-(25) are independent of each other, it is not necessary to dualize the sub-problems and a parallel computation strategy can be used to improve the solution efficiency.

III. LINEARIZATION OF THE PROPOSED MODEL
The proposed two-stage DRO model set up in Section II includes the absolute term in the confidence set (7), the quadratic term $f_g(P_{g,t}) = a_g P_{g,t}^2 + b_g P_{g,t} + c_g$ in generation cost (12). It is difficult to solve the proposed model with such non-linear terms and thereby a proper linearization technique is presented to solve the model.

A. LINEARIZATION OF CONFIDENCE SET
To handle the absolute term in confidence set (7), the binary auxiliary variables $z_n^+ z_n^-, y_n^+ y_n^-$ are introduced to transform

the 1-norm and ∞-norm constraints into a linear form. If denoted $P_n^+ = P_n - P_n^0$ and $P_n^- = P_n^0 - P_n$, the confidence set (7) could be rewritten by (26)-(33) [11].

$$\sum_{n=1}^{N} P_n^+ + P_n^- \leq \theta_1 \tag{26}$$

$$z_n^+ + z_n^- \leq 1 \tag{27}$$

$$0 \leq P_n^+ \leq z_n^+ \theta_1 \tag{28}$$

$$0 \leq P_n^- \leq z_n^- \theta_1 \tag{29}$$

$$P_n^+ + P_n^- \leq \theta_\infty \tag{30}$$

$$y_n^+ + y_n^- \leq 1 \tag{31}$$

$$0 \leq P_n^+ \leq y_n^+ \theta_\infty \tag{32}$$

$$0 \leq P_n^- \leq y_n^- \theta_\infty \tag{33}$$

B. LINEARIZATION OF GENERATOR COST
The quadratic generator cost is transformed into a linear form by using the piecewise linear technique [31] to divide generator power output into M segments, and the fuel cost $f_g(P_{g,t}) = a_g P_{g,t}^2 + b_g P_{g,t} + c_g$ can be transformed into (34)-(37).

$$f_g(P_{g,t}) = \sum_{m=1}^{M} K_{g,m} \eta_{g,t}^m + u_{g,t}\left(a_g \cdot P_g^{min2} + b_g P_g^{min} + c_g\right) \tag{34}$$

$$\text{s.t. } P_{g,t} = \sum_{m=1}^{M} \eta_{g,t}^m + u_{g,t} P_g^{min} \tag{35}$$

$$0 \leq \eta_{g,t}^m \leq u_{g,t} \eta_g^{max} \tag{36}$$

$$\eta_g^{max} = \left(P_g^{max} - P_g^{min}\right)/M \tag{37}$$

$K_{g,m}$ is the incremental cost of generator g at segment m, $\eta_{g,t}^m$ is the power output of generator g at segment m, η_g^{max} is the maximum power output of generator g.

IV. CCG ALGORITHM FOR SOLVING THE PROPOSED MODEL
In this section, the CCG algorithm is introduced to solve the proposed two-stage DRO model by decomposing it into a master problem and sub-problems, which are iteratively solved until the convergence condition is satisfied. For description convenience, the proposed DRO model is expressed in a compact matrix form in the following.

A. MASTER PROBLEM FORMATION OF DRO MODEL
The master problem (38) optimizes the generator ON-OFF status under the worst scenario identified by the sub-problem, and solutions of the master problem will be updated as the lower bound of the original DRO model.

$$\min_x a^T x + \max_{P_n \in D} \sum_{n=1}^{N} P_n \min_{y \in \Omega(x,w)} \left(b^T y\right)^n \tag{38}$$

$$\text{s.t. } Ax \leq d \tag{39}$$

where x stands for the first stage decision variables which are decided ahead of the operation including the generator ON-OFF status $u_{g,t}$; y is the second stage decision variable representing the generator power output $P_{g,t}$, the wind curtailment $\Delta w_{w,t}$, the load shedding $\Delta D_{d,t}$,

the charging/discharging power $p_{s,t}^{sd}/p_{s,t}^{sc}$ and SU charging/discharging status $I_{s,t}^{sc}/I_{s,t}^{sd}$; ξ is the wind power output subjected by the set D. The first part $a^T x$ of (38) represents the sum of generator start-up/shut-down cost corresponding to Eq. (8); the second part of (38) is the compact form of Eq. (14) for the generation cost, wind curtailment cost, load shedding cost, and charging/discharging cost, where $[*]^n$ is the optimal solution in scenario n. Constraint (39) is the compact form of (9)-(15).

B. SUB-PROBLEM FORMATION OF DRO MODEL
When the ON-OFF status of generators is determined in the master problem, the sub-problem will identify the worst probability distribution and provides an upper bound for the original DRO model.

$$\max_{P_n \in D} \sum_{n=1}^{N} P_n \min_{y \in \Omega(x,w)} \left(b^T y\right)^n \tag{40}$$

$$\text{s.t. } Bx + Cy^n + D\xi^n \leq f \tag{41}$$

where f is the corresponding vector and B, C, D are the corresponding coefficient matrices determined by (15)-(25).

It is evident that the sub-problem (40-41) is with a two-layer max-min structure, and is difficult to be solved directly. Due to the independence of representative scenarios in sub-problems, a dual-free parallel solution strategy is adopted in this paper [21]. Assume $k(n) = \min_{y \in \Omega(x,w)} \left(b^T y\right)^n$, model (40-41) can be transformed into (42)-(44).

$$V = \max_{P_n \in D} \sum_{n=1}^{N} P_n k(n) \tag{42}$$

$$\text{s.t. } k(n) = \arg\min \left(b^T y\right)^n \tag{43}$$

$$Bx + Cy^n + D\xi^n \leq f \tag{44}$$

Afterward, the above problem is solved by the following steps:

1) First, find the optimal solution for a single scenario n:

$$Bx + Cy^n + D\xi^n \leq f \tag{45}$$

$$x + Cy^n + D\xi^n \leq f \tag{46}$$

2) After obtaining $k(n)^*$ for N scenarios, optimize sub-problem (47).

$$\max_{P_n \in D} \sum_{n=1}^{N} P_n k(n)^* \tag{47}$$

If the sub-problem is infeasible, add the decision variable y_l^n and the feasible cut constraint (48) to the master problem.

$$Bx + Cy_l^n + D\xi^n \leq f \quad 1 \leq l \leq U \; 1 \leq n \leq N \tag{48}$$

where U means the number of feasible cuts.

If the sub-problem is feasible, add the decision variable y_l^n and the optimal cut (49)-(50) to the master problem.

$$\psi \geq \sum_{n=1}^{N} \left(P_n^l\right)^* \left(b^T y_l^n\right) \quad 1 \leq l \leq V \tag{49}$$

$$Bx + Cy_l^n + D\xi^n \leq f \quad 1 \leq l \leq V \; 1 \leq n \leq N \tag{50}$$

where V is the number of optimal cuts.

C. STEPS OF CCG ALGORITHM FOR PROPOSED TWO-STAGE DRO MODEL

1) Initialize the number of iteration as $k = 0$; set the lower bound as UB $= +\infty$ and the lower bound as LB$=0$;

2) Solve the main problem (51) with the constraint (52)

$$\min_{x,\psi} a^T x + \psi \qquad (51)$$

$$\text{s.t.} \begin{cases} Ax \leq d \\ \text{feasible cut} \\ \text{optimal cut} \end{cases} \qquad (52)$$

Get the optimal solution $x^*_{k+1}, \psi^*_{k+1}, (y^n_l)^*, \forall l, \forall n$, and update the lower bound LB $= a^T x^*_{k+1} + \psi^*_{k+1}$;

3) Solve the sub-problem

Based on the solutions x^*_{k+1} of the master problem, solve the sub-problem (45-46) in parallel to get the optimal value $k(n)^* 1 \leq n \leq N$ for all scenarios; afterward return $k(n)^*$ to equation (47) and calculate the optimal solution of the sub-problem as V^*_{k+1}, then update the upper bound UB $= \min\{UB, a^T x^*_{k+1} + V^*_{k+1}\}$, if the optimal solution doesn't exist, the feasible cut is formulated based on (48).

4) Check the convergence condition. If the condition $\left|\frac{LB-UB}{LB}\right| \leq \varepsilon$ is satisfied, terminate the program; otherwise, update $k = k+1$ and go to step 2).

V. CASE STUDY

A modified IEEE 39-bus system is used to test the proposed DRO model for wind farm and storage unit jointly operated power systems, where a wind farm and a storage unit are connected at nodes 29 and 14 respectively. Parameters of generators and SUs, the predicted wind power output and load demands are shown in TABLE 10-13 of the appendix. The prices of wind power curtailment and load shedding are 10 \$/MWh and 1000 \$/MWh respectively; the SU energy cycling price c_s is set as 30\$/MWh, and its charging/discharging power price c_{sd}/c_{sc} is 100\$/MWh. Then the IEEE 57-bus system and 118-bus system are carried out to verify the scalability of the proposed model for largescale systems. The data of the 57-bus system can be found in [32]. The wind farms are located at buses 39 and 45, while SUs are connected at buses 26 and 48. The data of the IEEE 118-bus system is available in http://motor. ece.iit.edu/data/ included 54 traditional generators and 186 transmission lines. The two wind farms are installed on buses 15 and 49. A SU with the same parameters used in the 39-bus system is connected at bus 69.

When historical data volume K of the uncertain wind power is 100 and the number of scenarios N is set as 10, the optimized ON-OFF status of the 10 generators are shown in Fig. 1 with the corresponding power output demonstrated in Fig. 2 for one representative scenario.

To verify the effectiveness of the proposed DRO model, the SO model [33] and RO model [34] are also solved for comparisons, and the corresponding costs are detailed in Table 1. In specific, the second-stage problem of RO
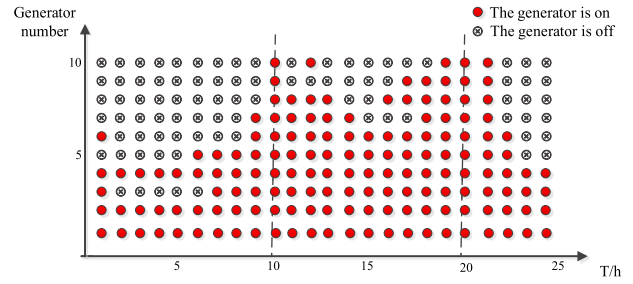

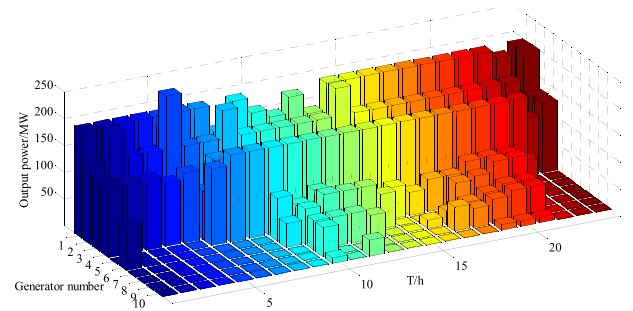**FIGURE 1.** Optimized ON and OFF status of 10 generators.

FIGURE 2. Output power of 10 generators for one scenario.

TABLE 1. Comparisons of DRO, RO and SO solutions.

The calculation result	DRO	RO	SO
iterations	3	3	1
wind curtailment cost/\$	460.5	0	553.1
load shedding cost/\$	268348.9	271915.2351	264420.5
energy storage cost/\$	38435.3	21576.13712	494984.2
Total cost/\$	792622.1	833382.2244	788345.4

model include the binary variables which are not supported by the strong dually, thus the problem is solved by nested-C&CG [35]. As shown in Table 1, the total cost of DRO model is lower than RO, but higher than SO. This is because the wind power output in SO follows a normal distribution, and it is only part of the possible distribution of the confidence set of DRO; while the RO model intends to get a solution under the worst scenario for a given uncertain set of wind power output, so DRO model arrives at a compromise solution compared with the RO and SO models.

To verify the impact of wind power historical data volume on system total cost, the number of historical data K is varied from 10 to 2000, and the corresponding system total cost solved by the DRO is shown in Fig 3. With a growing number K of wind power historical data, the system total cost of DRO under the combined 1-norm and ∞-norm confidence set continues to decrease. This is because the probability deviations of the uncertainty variables θ_1 and θ_∞ decrease accordingly with the growing number of historical data, resulting in decreased fluctuations of wind power output and consequently the system total cost is reduced.

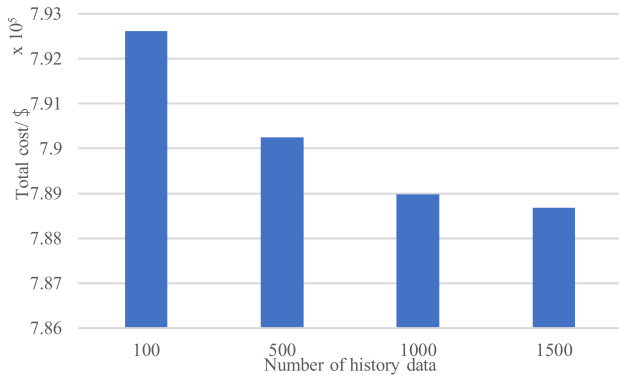In order to investigate the impacts of the confidence level of wind power uncertain output on system total cost, keep α_∞

FIGURE 3. Total cost for varied number of wind power historical data.

as 0.95 and change α_1 from 0.5 to 0.1, the system total cost constrained by the single ∞-norm and the 1-norm united ∞-norm confidence set is given in Table 2. While α_1 remains at 0.99, the total cost under different confidence set with changed α_∞ is listed in Table 3.

TABLE 2. Cost Comparisons between ∞-norm confidence set and under 1-norm united ∞-norm confidence set.

α_1	Total cost/$	
	∞-norm confidence set	1-norm united ∞-norm confidence set
0.7	792654.3	792578.5
0.5	792654.3	792576.1
0.2	792654.3	792558.6

TABLE 3. Cost Comparisons between 1-norm confidence set and under 1-norm united ∞-norm confidence set.

α_∞	Total cost/$	
	1-norm confidence set	1-norm united ∞-norm confidence set
0.8	792614.9	792588.5
0.4	792614.9	792574.2
0.1	792614.9	792551.4

As shown in Table 2-3, the wind farm and SU jointed operation model under the 1-norm united ∞-norm confidence set exhibits the lowest total cost compared with the model with the separated 1-norm or ∞-norm confidence set. The underlying reason is that for the combined 1-norm and ∞-norm confidence set, the uncertainty of the wind power output is decreased and alleviated, resulting in a smaller scale of wind curtailment, load shedding and charging/discharging power to cope with the uncertainties, and thus the system total cost is reduced. Furthermore though the ∞-norm confidence level α_∞ for table 2 equals the 1-norm confidence α_1 for table 3, the total cost under the 1-norm confidence set is larger than that of ∞-norm confidence set. As θ_1 is larger than θ_∞ for the same confidence level ($\alpha_1 = \alpha_\infty$) according to Eqs. (5)-(6), the 1-norm confidence set is more conservative than the ∞-norm confidence set. What's more, with the decreased

TABLE 4. Total cost under different probabilistic distributions and confidence levels of α_∞.

Confidence level α_∞	Total cost/$		
	Beta	Laplace	T
0.9	818228.8	798807.4	785116.6
0.7	818122.3	798705.6	785099.5
0.5	818072.5	798658.1	785072.3
0.2	818026	798614.6	785059.7

TABLE 5. Total cost under different probabilistic distributions and confidence levels of α_1.

Confidence level α_1	Total cost/$		
	Beta	Laplace	T
0.8	818161.2	798747.5	818161.2
0.6	818093.6	798676.5	818093.6
0.4	818054.1	798638.8	818054.1
0.1	818014.6	798605.0	818014.6

confidence level α_∞ or α_1, the system total cost decreases accordingly, because when the confidence level goes down, the confidence set becomes smaller and is less conservative.

Table 4 and Table 5 further demonstrate the system total cost for different probabilistic distributions with varying confidence levels. It shows that for any of the probabilistic distribution, the system total cost always decreases with the reduced confidence level. This implies that the reduced confidence level leads to the decreased uncertainty of wind power output, and thus requires a smaller amount of flexible power output of generators and fast-response charging/discharging power of SU to balance the fluctuation of wind power. What's more, the model is distribution-free and can be used for wind power uncertainties satisfying various probabilistic distributions.

TABLE 6. The comparison between the joint system and wind farm system.

Cost	Wind farm	Joint system
Load shedding cost/$	370337.1	268348.9
Wind curtailment cost/$	460.6	460.5
Total cost/$	867762.0	792622.1

In order to validate the effectiveness of SU, the independent operation of a wind farm is compared with the proposed wind farm and SU jointly operated model. With confidence levels α_1 and α_∞ kept at 0.9, the load shedding cost, wind curtailment cost, and system total cost are demonstrated in Table 6. From Table 6, compared with the wind farm independent operation mode without any SU, the load shedding cost, the wind curtailment cost and system total cost significantly decreased for the wind farm and SU jointed operation model. As SU could perform charging and discharging properly to reduce wind curtailment and load shedding, SU effectively improves wind power accommodation level. For the confidence level fixed as 0.95 and N as 10, the detailed charging/discharging power and SOC of SU during 24 hours are shown in Fig.4 and Fig.5. When the system load demand is at the
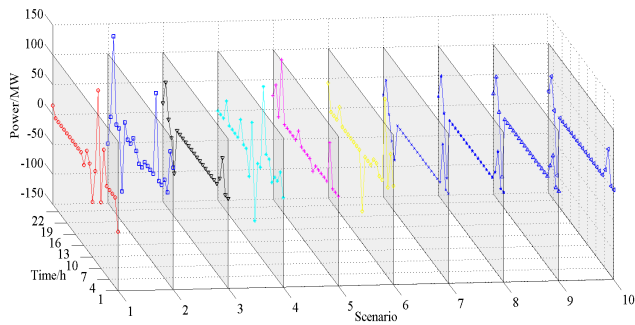
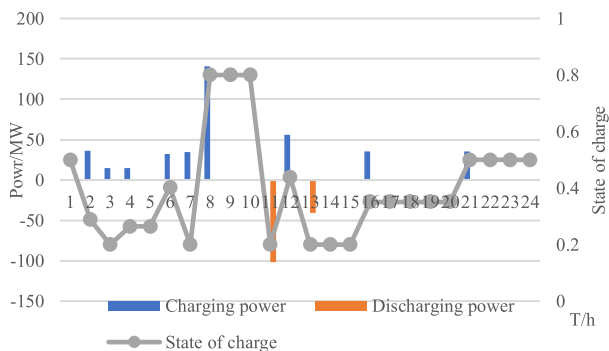**FIGURE 4.** SU Charging/Discharging power during 24 hours.

FIGURE 5. Charging/discharging power and SOC of SU.

TABLE 7. Costs under varied charging/ discharging power limits.

Cost/ $	Value of $p_{max}^{sc}, p_{max}^{sd}$/MW				
	30	40	50	80	100
Total cost	823555	808820	794088	792622	792627
Load shedding cost	310349	290349	270349	268349	268349
Energy storage cost	14304	19073	23841	24318	24318

FIGURE 7. Costs for different SU capacity.

valley while wind power output is around the peak during 2:00-4:00, SU is properly charged; while for the peak load and valley wind power period 11:00-12:00, SU displays reasonable discharging behaviors. These results indicate that the SU could reduce the load peak-valley variations and ensures the smooth operation of conventional generators with lower operation costs, and thus SU effectively explores the energy shift arbitrage to reduce the system total cost.
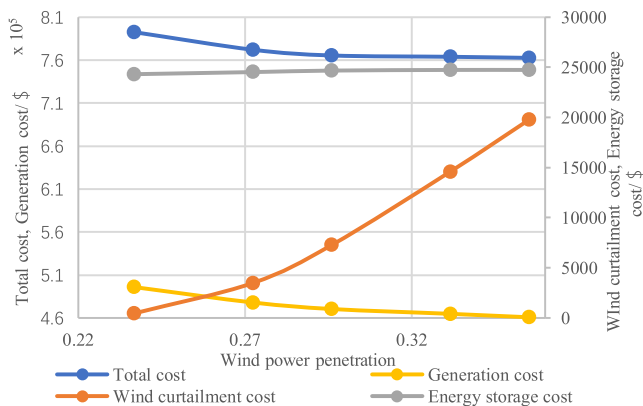

FIGURE 6. Costs with different wind power penetration levels.

To investigate the influence of different wind power penetration levels on the system operation cost, the simulations are conducted for varied wind power penetration increasing from 0.1 to 0.3, while the energy storage cost, the load shedding cost, and the system operation costs, etc. are shown in Fig.6 accordingly.
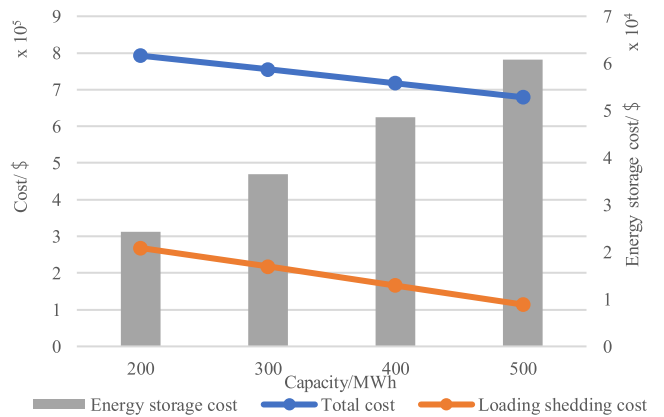
In Fig.6, with the higher wind power penetration, the units operation cost, the loading shedding cost and total cost are all decreased. Because of the more wind power output, the system would support more load demand without running a large number of conventional generators to guarantee the power balance. As for the wind curtailment cost, it maintains zero at first which means the system has fully accommodated wind power output. And then as the wind power penetration increases, the system needs to abandon a certain amount of wind power output thus leading to the increase of wind curtailment cost. The energy storage cost tends to grow and then stay saturated as the wind power penetration rises. This is because the increased wind power penetration brings more uncertainty, the energy storage unit performs more reasonable charging/discharging behaviors to deal with uncertainty. But when the wind power penetration reaches 0.33, the system cannot absorb any more uncertain energy due to the capacity of energy storage exhausted.

Table 7 shows the costs under different charging/ discharging power limits. As the unit maximum charging/ discharging power increases, the total cost and loading shedding cost are reduced at first. At the same time, the energy storage cost becomes higher. This is because the increased unit charging/discharging power of SU enables the system to absorb more wind power and reduce the loading shedding amount. But when energy storage reaches a saturated state with exhausted energy capacity, further increasing the SU maximum charge and discharging power can no longer bring higher economic benefits.

TABLE 8. Computational efficiency comparisons of two methods.

Model	System	Variables number		Constraints number		Time(s)
		General expression	Number	General expression	Number	
RO	39-bus	$3G \times T + (G + 5 \times S + W + D) \times T$	2040	$5G \times T + (4G + 1 + 6 \times S + K + W + D) \times T$	4492	2133
	57-bus		2520		5616	3201
	118-bus		8160		19152	15126
DRO	39-bus	$3G \times T + (G + 5 \times S + W + D) \times T \times N$	13920	$5G \times T + (4G + 1 + 6 \times S + K + W + D) \times T \times N$	33120	243
	57-bus		18918		45460	358
	118-bus		46608		133200	1087

TABLE 9. Dispatching cost of the 57-bus system and 118-bus system.

Cost/ $	57-bus system		118-bus system	
	RO	DRO	RO	DRO
Wind curtailment cost	2135.9	3278.8	0	0
Load shedding cost	102580	98178.9	0	0
Energy storage cost	28439.3	34517.6	24000	36000
Total cost	555140.4	521500.5	224372.4	2057345.6

TABLE 10. Load demands in 24 hours.

Time (h)	Load (MW)	Time (h)	Load (MW)
1	930	13	1400
2	830	14	1300
3	750	15	1200
4	710	16	1050
5	800	17	1000
6	980	18	1100
7	1150	19	1200
8	1200	20	1400
9	1300	21	1300
10	1400	22	1100
11	1450	23	950
12	1500	24	880

TABLE 11. Operation limits of 10 generators.

unit	P_g^{max}(MW)	P_g^{min}(MW)	R_{Ug}/R_{Dg}	T_g^{on}/T_g^{off}(h)
1	455	150	120	8
2	450	150	120	8
3	130	20	40	5
4	130	20	40	5
5	162	25	50	6
6	80	20	20	3
7	85	25	20	3
8	55	10	10	1
9	55	10	10	1
10	55	10	10	1

TABLE 12. Cost parameters of 10 generators.

unit	a_g $/MWh^2	b_g $/MWh	c_g $/h	Start-up cost ($)	Shut-down cost ($)
1	0.00048	16.19	1000	4500	100
2	0.00031	17.26	970	5000	100
3	0.002	16.6	700	550	100
4	0.00211	16.5	680	560	100
5	0.00398	19.7	450	900	100
6	0.000712	22.26	370	170	100
7	0.00079	27.74	480	260	100
8	0.00413	25.92	660	30	100
9	0.00222	27.27	665	30	100
10	0.00173	27.79	670	30	100

TABLE 13. SU Operation parameters.

Parameter	Value	Parameter	Value
$p_{max}^{sc}, p_{max}^{sd}$(MW)	200	Q_{rate}(MWh)	200
$p_{min}^{sc}, p_{min}^{sd}$(MW)	15	η_c, η_d	0.85
SOC_{min}, SOC_{max}	0.8,0.2	SOC_0	0.5

In Fig.7, the system total cost is also investigated for different capacities of SU. As shown in Fig.7, the system total cost decreases as the SU capacity increases due to its enhanced energy shift capability. Moreover, the larger SU capacity is helpful to reduce the loading shedding cost. Since the rapid charging/discharging capability of SU could enhance the joint system operation flexibility, a larger SU alleviates the load shedding to balance wind power fluctuations.

To verify the computational performance, the comparison is presented in TABLE 8. It can be observed that the computation time taken by the DRO model is always lower than those of the RO algorithm for the three systems. Concerning

DRO, when the system scale is enlarged with a growing number of decision variables and constraints, the time cost of DRO is slightly increased but still satisfied for the day-head dispatching application. Thus it can be concluded that the proposed algorithm is computationally efficient.

We further test the scalability of the approach for large-scale systems. The operation costs of DRO and RO for the 57-bus and 118-bus systems are listed in Table 9, and it is clear that the DRO model has a lower total operation cost, which implies that the DRO approach could provide a very economic operation strategy for different scale systems.

VI. CONCLUSION

In this paper, the uncertain wind power is first modeled by the combined 1-norm and ∞-norm confidence set, and then a two-stage distributionally robust optimization model is proposed for wind farm and storage unit jointly operated power system. Afterward, the CCG decomposition algorithm is applied to efficiently solve the presented model. Simulation validates that, 1) The proposed distributionally robust optimization model could make a compromise solution between RO and SO model; 2) With the increased confidence level of the uncertain wind power output, the joint system needs to dispatch more output power of flexible generators, and wind curtailment as well as load shedding, the system total cost thus increases accordingly; 3) SU could effectively reduce the cost of wind power curtailment and load shedding as well as system total cost through properly charging and discharging behaviors. This paper mainly takes into account the active power-related constraints, and the reactive power constraints which may also have influences on the optimal solution would be considered in the future for establishing a refined model.

APPENDIX

See Tables 10–13.

REFERENCES

[1] M. Yang, S. Fan, and W.-J. Lee, "Probabilistic short-term wind power forecast using componential sparse Bayesian learning," *IEEE Trans. Ind. Appl.*, vol. 49, no. 6, pp. 2783–2792, Nov. 2013.

[2] Y. Chen, Z. Zhang, H. Chen, and H. Zheng, "Robust UC model based on multi-band uncertainty set considering the temporal correlation of wind/load prediction errors," *IET Gener., Transmiss. Distrib.*, vol. 14, no. 2, pp. 180–190, Jan. 2020.

[3] Z. Zhang, Y. Chen, X. Liu, and W. Wang, "Two-stage robust security-constrained unit commitment model considering time autocorrelation of wind/load prediction error and outage contingency probability of units," *IEEE Access*, vol. 7, pp. 25398–25408, 2019.

[4] Z. Zhang, Y. Chen, J. Ma, X. Liu, and W. Wang, "Two-stage robust security constrained unit commitment considering the spatiotemporal correlation of uncertainty prediction error," *IEEE Access*, vol. 7, pp. 22891–22901, 2019.

[5] X. Lu, K. W. Chan, S. Xia, X. Zhang, G. Wang, and F. Li, "A model to mitigate forecast uncertainties in distribution systems using the temporal flexibility of EVAs," *IEEE Trans. Power Syst.*, vol. 35, no. 3, pp. 2212–2221, May 2020.

[6] X. Lu, S. Xia, W. Gu, K. W. Chan, and M. Shahidehpour, "Two-stage robust distribution system operation by coordinating electric vehicle aggregator charging and load curtailments," *Energy*, vol. 226, Jul. 2021, Art. no. 120345.

[7] X. Lu, K. W. Chan, S. Xia, M. Shahidehpour, and W. H. Ng, "An operation model for distribution companies using the flexibility of electric vehicle aggregators," *IEEE Trans. Smart Grid*, vol. 12, no. 2, pp. 1507–1518, Mar. 2021.

[8] P. Xiong, P. Jirutitijaroen, and C. Singh, "A distributionally robust optimization model for unit commitment considering uncertain wind power generation," *IEEE Trans. Power Syst.*, vol. 32, no. 1, pp. 1–11, Jan. 2017.

[9] C. Liu, C. Lee, H. Chen, and S. Mehrotra, "Stochastic robust mathematical programming model for power system optimization," *IEEE Trans. Power Syst.*, vol. 31, no. 1, pp. 821–822, Jan. 2016.

[10] Y. Chen, Q. Guo, H. Sun, Z. Li, W. Wu, and Z. Li, "A distributionally robust optimization model for unit commitment based on Kullback–Leibler divergence," *IEEE Trans. Power Syst.*, vol. 33, no. 5, pp. 5147–5160, Sep. 2018.

[11] W. Wei, F. Liu, and S. Mei, "Distributionally robust co-optimization of energy and reserve dispatch," *IEEE Trans. Sustain. Energy*, vol. 7, no. 1, pp. 289–300, Jan. 2017.

[12] Z. Li, W. Wu, B. Zhang, and X. Tai, "Kullback–Leibler divergence-based distributionally robust optimisation model for heat pump day-ahead operational schedule to improve PV integration," *IET Gener., Transmiss. Distrib.*, vol. 12, no. 13, pp. 3136–3144, Jul. 2018.

[13] C. Duan, L. Jiang, W. Fang, J. Liu, and S. Liu, "Data-driven distributionally robust energy-reserve-storage dispatch," *IEEE Trans. Ind. Informat.*, vol. 14, no. 7, pp. 2826–2836, Jul. 2018.

[14] Z. Wang, Q. Bian, H. Xin, and D. Gan, "A distributionally robust co-ordinated reserve scheduling model considering CVaR-based wind power reserve requirements," *IEEE Trans. Sustain. Energy*, vol. 7, no. 2, pp. 625–636, Apr. 2016.

[15] Y. Zhang, J. Le, F. Zheng, Y. Zhang, and K. Liu, "Two-stage distributionally robust coordinated scheduling for gas-electricity integrated energy system considering wind power uncertainty and reserve capacity configuration," *Renew. Energy*, vol. 135, pp. 122–135, May 2019.

[16] X. Xu, Z. Yan, M. Shahidehpour, Z. Li, M. Yan, and X. Kong, "Data-driven risk-averse two-stage optimal stochastic scheduling of energy and reserve with correlated wind power," *IEEE Trans. Sustain. Energy*, vol. 11, no. 1, pp. 436–447, Jan. 2020.

[17] C. Zhao and Y. Guan, "Data-driven stochastic unit commitment for integrating wind generation," *IEEE Trans. Power Syst.*, vol. 31, no. 4, pp. 2587–2596, Jul. 2016.

[18] G. Darivianakis, A. Eichler, R. S. Smith, and J. Lygeros, "A data-driven stochastic optimization approach to the seasonal storage energy management," *IEEE Control Syst. Lett.*, vol. 1, no. 2, pp. 394–399, Oct. 2017.

[19] A. Bagheri, J. Wang, and C. Zhao, "Data-driven stochastic transmission expansion planning," *IEEE Trans. Power Syst.*, vol. 32, no. 5, pp. 3461–3470, Sep. 2017.

[20] K. Pan and Y. Guan, "Data-driven risk-averse stochastic self-scheduling for combined-cycle units," *IEEE Trans. Ind. Informat.*, vol. 13, no. 6, pp. 3058–3069, Dec. 2017.

[21] T. Ding, Q. Yang, Y. Yang, C. Li, Z. Bie, and F. Blaabjerg, "A data-driven stochastic reactive power optimization considering uncertainties in active distribution networks and decomposition method," *IEEE Trans. Smart Grid*, vol. 9, no. 5, pp. 4994–5004, Sep. 2018.

[22] Q. Bian, H. Xin, Z. Wang, D. Gan, and K. P. Wong, "Distributionally robust solution to the reserve scheduling problem with partial information of wind power," *IEEE Trans. Power Syst.*, vol. 30, no. 5, pp. 2822–2823, Sep. 2015.

[23] X. Chen, W. Wu, B. Zhang, and C. Lin, "Data-driven DG capacity assessment method for active distribution networks," *IEEE Trans. Power Syst.*, vol. 32, no. 5, pp. 3946–3957, Sep. 2017.

[24] C. Zhao and R. Jiang, "Distributionally robust contingency-constrained unit commitment," *IEEE Trans. Power Syst.*, vol. 33, no. 1, pp. 94–102, Jan. 2018.

[25] E. P. Mohajerin and D. Kuhn, "Data-driven distributionally robust optimization using the Wasserstein metric: Performance guarantees and tractable reformulations," *Math. Program.*, vol. 171, pp. 66–115, Sep. 2018.

[26] X. Wu, S. Qi, Z. Wang, C. Duan, X. Wang, and F. Li, "Optimal scheduling for microgrids with hydrogen fueling stations considering uncertainty using data-driven approach," *Appl. Energy*, vol. 253, Nov. 2019, Art. no. 113568.

[27] X. Shen, J. Liu, and H. Ruan, "A distributionally robust optimization model for the decomposition of contract electricity considering uncertainty of wind power," in *Proc. IEEE Int. Conf. Autom., Electron. Electr. Eng. (AUTEEE)*, Nov. 2018, pp. 64–68.

[28] Y. Shui, H. Gao, J. Wang, Z. Wei, and J. Liu, "A data-driven distributionally robust coordinated dispatch model for integrated power and heating systems considering wind power uncertainties," *Int. J. Elect. Power*, vol. 104, pp. 255–258, Jan. 2019.

[29] H. Beltran, I. Tomas Garcia, J. C. Alfonso-Gil, and E. Perez, "Levelized cost of storage for Li-ion batteries used in PV power plants for ramp-rate control," *IEEE Trans. Energy Convers.*, vol. 34, no. 1, pp. 554–561, Mar. 2019.

[30] S. Xia, K. W. Chan, X. Luo, S. Bu, Z. Ding, and B. Zhou, "Optimal sizing of energy storage system and its cost-benefit analysis for power grid planning with intermittent wind generation," *Renew. Energy*, vol. 122, pp. 472–486, Jul. 2018.

[31] J. Garcia-Gonzalez, R. M. R. de la Muela, L. M. Santos, and A. M. Gonzalez, "Stochastic joint optimization of wind generation and pumped-storage units in an electricity market," *IEEE Trans. Power Syst.*, vol. 23, no. 2, pp. 460–468, May 2008.

[32] L. L. Freris and A. M. Sasson, "Investigation of the load-flow problem," *Elect. Eng. Proc. Inst. Elect. Eng.*, vol. 115, no. 10, pp. 1459–1470, 1968.

[33] P. Carpentier, G. Gohen, J. C. Culioli, and A. Renaud, "Stochastic optimization of unit commitment: A new decomposition framework," *IEEE Trans. Power Syst.*, vol. 11, no. 2, pp. 1067–1073, May 1996.

[34] D. Bertsimas, E. Litvinov, X. A. Sun, J. Zhao, and T. Zheng, "Adaptive robust optimization for the security constrained unit commitment problem," *IEEE Trans. Power Syst.*, vol. 28, no. 1, pp. 52–63, Feb. 2013.

[35] C. Wang, W. Wei, J. Wang, F. Liu, F. Qiu, C. M. Correa-Posada, and S. Mei, "Robust defense strategy for gas-electric systems against malicious attacks," *IEEE Trans. Power Syst.*, vol. 32, no. 4, pp. 2953–2965, Jul. 2017.

YUEHUI HUANG (Senior Member, IEEE) received the B.S. and M.S. degrees from Xi'an Jiaotong University, in 2002 and 2005, respectively, and the Ph.D. degree from the Department of Electronic and Information Engineering, The Hong Kong Polytechnic University, in 2008. She is currently with CEPRI, Beijing. Her research interests include renewable generation integration and its dispatch and operation technology.

XIAOYUN WU received the master's degree from Harbin Institute of Technology, Harbin, China, in 2009. He currently works with Opto-Electronics Information Science and Engineering, Huaihua University. His research interests include distributed generation and microgrid technology.

PANPAN LI (Graduate Student Member, IEEE) received the B.S. degree from Zhengzhou University, Zhengzhou, China, in 2019. She is currently pursuing the M.S. degree with North China Electric Power University, Beijing, China. Her current research interest includes low-carbon economic dispatch of power systems.

LIANGYUN SONG received the B.S. degree from Nanchang University, Nanchang, China, in 2018. She is currently pursuing the M.S. degree with North China Electric Power University, Beijing, China. Her current research interests include stochastic optimization and robust control of power systems.

XI LU received the B.Sc. degree in electrical engineering from North China Electric Power University, Beijing, China, in 2015, and the Ph.D. degree from The Hong Kong Polytechnic University, Hung Hom, Hong Kong, in 2020. He is currently with the School of Electrical Engineering, Southeast University, Nanjing. His research interests include the application of robust optimization and distributionally robust optimization in power system operation.

JIXIAN QU received the B.S. degree from Wuhan University, Wuhan, China, in 2013, and the master's degree from China Electrical Power Research Institute (CEPRI), Beijing, in 2016. She is currently working as an Engineer with CEPRI. Her research interests include energy technology strategy, new energy planning, and grid-connected analysis.

SHIWEI XIA (Senior Member, IEEE) received the Ph.D. degree from The Hong Kong Polytechnic University, Hung Hom, Hong Kong, in 2015. He is currently with the State Key Laboratory of Alternate Electrical Power System with Renewable Energy Sources, North China Electric Power University, Beijing, China, and with the Yangzhong Intelligent Electrical Research Center, North China Electric Power University. His research interests include security and risk analysis for power systems with renewables, distributed optimization, and control of AC–DC distribution grid.

● ● ●